Int. J. Radiation Oncology Biol. Phys., Vol. ■, No. ■, pp. 1–8, 2011

0360-3016/$ - see front matter

ELSEVIER

doi:10.1016/j.ijrobp.2011.03.035

CLINICAL INVESTIGATION

DENTALMAPS: AUTOMATIC DENTAL DELINEATION FOR RADIOTHERAPY PLANNING IN HEAD-AND-NECK CANCER

Juliette Thariat, M.D.,* Liliane Ramus, M.Sc.,†‡ Philippe Maingon, M.D.,§ Guillaume Odin, M.D., Ph.D.,‖ Vincent Gregoire, M.D. Ph.D.,¶ Vincent Darcourt, M.D.,# Nicolas Guevara, M.D. Ph.D.,‖ Marie-Helene Orlanducci, M.D.,** Serge Marcie, Ph.D.,* Gilles Poissonnet, M.D.,†† Pierre-Yves Marcy, M.D.,‡‡ Alex Bozec, M.D.,†† Olivier Dassonville, M.D.,†† Laurent Castillo, M.D.,‖ Francois Demard, M.D.,†† Jose Santini, M.D.,†† and Gregoire Malandain, Ph.D.‡

*Department of Radiation Oncology/Institut de biologie et developpement du cancer (IBDC) centre national de la recherche scientifique (CNRS) unite mixte de recherche (UMR) 6543, #Department of Radiation Oncology–Dentistry, and ‡‡Department of Radiology, Cancer Center Antoine-Lacassagne, University of Nice Sophia-Antipolis, Nice Cedex, France; †DOSIsoft, Cachan, France; ‡INRIA (Institut National de Recherche en Automatique et en Automatique)–Asclepios Research Project, Sophia-Antipolis, France; §Department of Radiation Oncology, Centre Georges-François Leclerc, Dijon Cedex, France; ‖Department of Head-and-Neck Surgery, Centre Hospitalier Universitaire–Institut Universitaire de la Face et du Cou, Nice Cedex, France; ¶Department of Radiation Oncology, St.-Luc University Hospital, Brussels, Belgium; **Department of Odontology, CHU, Nice, France; and ††Department of Head-and-Neck Surgery, Cancer Center Antoine-Lacassagne–Institut Universitaire de la Face et du Cou, Nice Cedex, France

Purpose: To propose an automatic atlas-based segmentation framework of the dental structures, called Dentalmaps, and to assess its accuracy and relevance to guide dental care in the context of intensity-modulated radiotherapy.

Methods and Materials: A multi-atlas–based segmentation, less sensitive to artifacts than previously published head-and-neck segmentation methods, was used. The manual segmentations of a 21-patient database were first deformed onto the query using nonlinear registrations with the training images and then fused to estimate the consensus segmentation of the query.

Results: The framework was evaluated with a leave-one-out protocol. The maximum doses estimated using manual contours were considered as ground truth and compared with the maximum doses estimated using automatic contours. The dose estimation error was within 2-Gy accuracy in 75% of cases (with a median of 0.9 Gy), whereas it was within 2-Gy accuracy in 30% of cases only with the visual estimation method without any contour, which is the routine practice procedure.

Conclusions: Dose estimates using this framework were more accurate than visual estimates without dental contour. Dentalmaps represents a useful documentation and communication tool between radiation oncologists and dentists in routine practice. Prospective multicenter assessment is underway on patients extrinsic to the database. © 2011 Elsevier Inc.

Atlas, Automatic dental segmentation, Radiotherapy planning, Osteoradionecrosis, Dentist.

INTRODUCTION

Dentate patients who undergo irradiation of the head and neck (H&N) suffer from various degrees of xerostomia and subsequent dental decay, with cases of postextraction osteoradionecrosis (ORN) (1) and implant failure (2–4). Preservation of dental structures requires long-term compliance with fluoride custom trays (*i.e.*, these should be used at least 5 days per week for daily 5-min applications) or substitutes like fluoride toothpaste (1350 ppm or more) (5–7). Dental decay is direct through irradiation of the

Reprint requests: Juliette Thariat, M.D., Department of Radiation Oncology/IBDC CNRS UMR 6543, Cancer Center Antoine-Lacassagne, University of Nice Sophia-Antipolis, 33 Av. Valombrose, 06189 Nice Cedex 2, France. Tel: (+33) 492031270; Fax: (+33) 492031570; E-mail: jthariat@hotmail.com

Presented at the 52nd Annual Meeting of the American Society for Radiation Oncology, October 31–November 4, 2010, San Diego, CA.

This work was supported by a grant from the 'Provence Alpes Cote d'Azur Canceropole and in part by the Association Nationale de la Recherche et de la Technologie. L.R. was supported by Dosisoft and ANRT (Association Nationale de la Recherche et de la Technologie) for her Ph.D.

J.T. and L.R. are co-first authors.

Conflict of interest: none.

Received Dec 20, 2010, and in revised form March 4, 2011. Accepted for publication March 12, 2011.

surrounding bone at the level of dental roots (8, 9) or indirect through damage to the salivary glands and mucosa. Recent techniques like intensity-modulated radiotherapy (IMRT), modulated arc therapy, tomotherapy, and stereotactic radiotherapy allow for steep dose gradients and preservation of the parotid glands (10, 11). The impact of these techniques on dental structures has been poorly studied. Dental dose risk levels have been empirically estimated on dosimetric data lacking mandibular, maxillary, and dental contours. It has therefore been a difficult task for radiation oncologists to provide accurate dose estimations to dentists planning postirradiation extractions (Fig. 1). Of note, dental dose is currently assessed on rough estimates of dose to underlying bone from retrospective dosimetric data that can be neither accurate nor reproducible even with two-dimensional (2D) irradiation. Dose distributions are even less predictable with highly conformal radiation techniques (*i.e.*, more complex dose distributions). Additionally, because of the multiplicity of beam paths with these modalities, nondelineated structures like anterior teeth may receive higher doses than those planned with 2D irradiation (12) (Fig. 1).

Manual delineation of mandibular and maxillary bones and teeth is tedious, time-consuming, and basically impossible in routine practice. Automatic segmentation would allow generation of tooth-by-tooth dose–volume histograms (DVHs). These would be useful to provide dental doses to dentists who want to pull teeth (particularly to assess the risk of ORN) or to place dental implants, because both procedure risks are known to be correlated with dose. The only realistic method to assess doses to teeth on planning CT should be based on automatic segmentation tools. A segmentation framework called Dentalmaps was proposed to segment each dental structure individually in H&N patients undergoing irradiation. The accuracy and relevance of Dentalmaps to estimate the dose to each tooth and to guide dental care were assessed for patients undergoing IMRT.

METHODS AND MATERIALS

Automatic dental segmentation was performed using a multi-atlas framework based on a bank of manually delineated CT images.

Data acquisition

Computed Tomography (CT) data (2.5-mm-thick slices) of 21 H&N dentate cancer patients were used. Patients with more than six missing teeth or significant dental artifacts were excluded. A radiation oncologist manually contoured the maxilla, mandible, and all dental structures (2 h on average). A 800–2500 Hounsfield unit windowing level was used. Other volumes were delineated as usual. Each image of the database was symmetrized with respect to its midsagittal plane, as well as its associated manual segmentation. This yielded $N = 42$ manually delineated images, referred to as "training data."

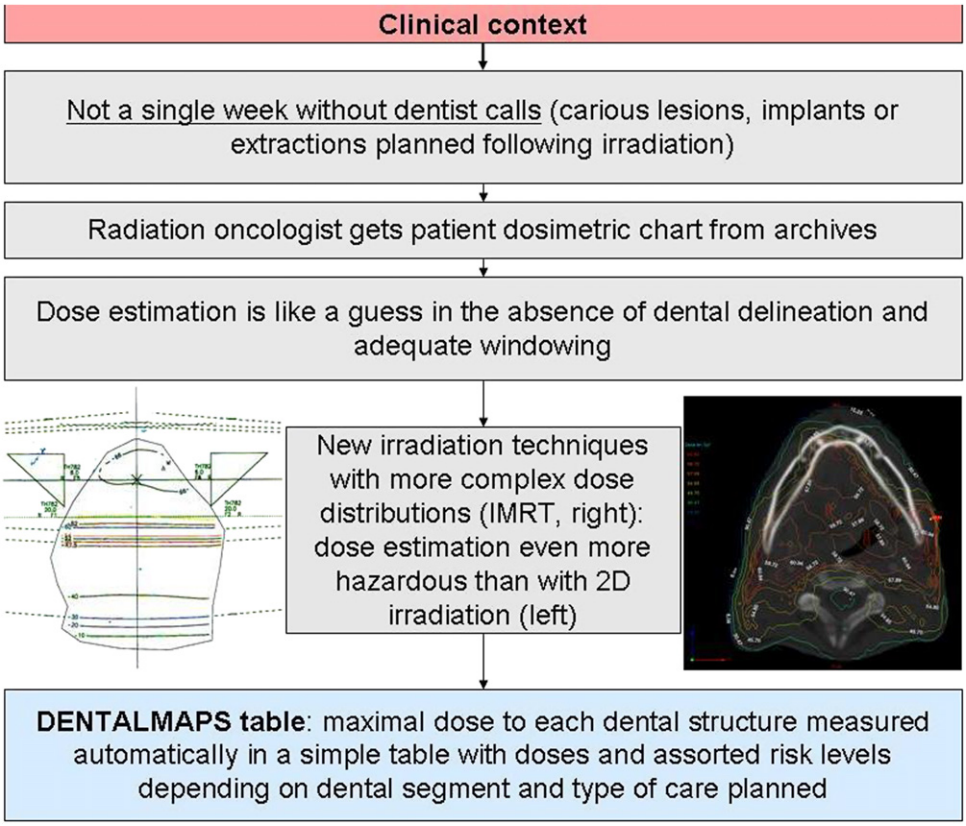

Fig. 1. Clinical context and potential routine use of our framework Dentalmaps. IMRT = intensity-modulated radiotherapy; 2D = two-dimensional.

Atlas-based segmentation strategy

There are different ways to exploit the training data and yield an estimation of the segmentation of a new query image. The first is to construct and use an average atlas. It is based on the three following successive steps: (*1*) construction of an average atlas (average-intensity image and its corresponding average segmentation), (*2*) nonlinear registration between the query and the average-intensity image, and (*3*) deformation of the average segmentation on the query. The atlas construction (step 1) was tested using a previously proposed framework dedicated to organs at risk (OARs) and H&N lymph node level segmentation (13, 14). However, the resulting average-intensity image was blurred around teeth owing to artifacts in the training images, which limited the capabilities of accurate nonlinear registration (and therefore segmentation) around dental structures, and in particular at the boundaries between two neighboring teeth. We thus used an alternative approach, called "multi-atlas–based segmentation," as described hereafter. First, we registered each training image with the query directly and deformed the segmentations of N training images onto the query. As nonlinear registration, we used a block-matching nonlinear registration algorithm (15). This provided a set of N candidate segmentations of the query, which were then combined to estimate the final query segmentation. For the combination step, we considered each tooth independently from the others. We computed a probability map from the candidate segmentations for each tooth, smoothed it with a Gaussian filter, and thresholded it to obtain a binary dental segmentation. The optimal values for the standard deviation of the Gaussian filter and the threshold were chosen to maximize segmentation accuracy through a leave-one-out procedure on the entire database. We then applied a morphologic closing and extracted the main connected component for each binary segmentation, independently. To make up for possible overlaps between two neighboring teeth, we removed overlap areas in the binary structures and then computed a Skeleton by Influence Zones of the resulting nonoverlapping components into the mask of the overlapping teeth. At the end, the pipeline provided nonoverlapping, contiguous, and smooth binary structures for all the teeth.

These contours were used to estimate the maximum dose received for each tooth. To consider possible segmentation errors due to intrinsic anatomic variability or due to the small dental size compared with the CT slice thickness, and to avoid underestimation of the maximum dose, three-dimensional (3D) morphologic expansions can potentially be added to automatic contours (overview of the method is shown in Fig. 2).

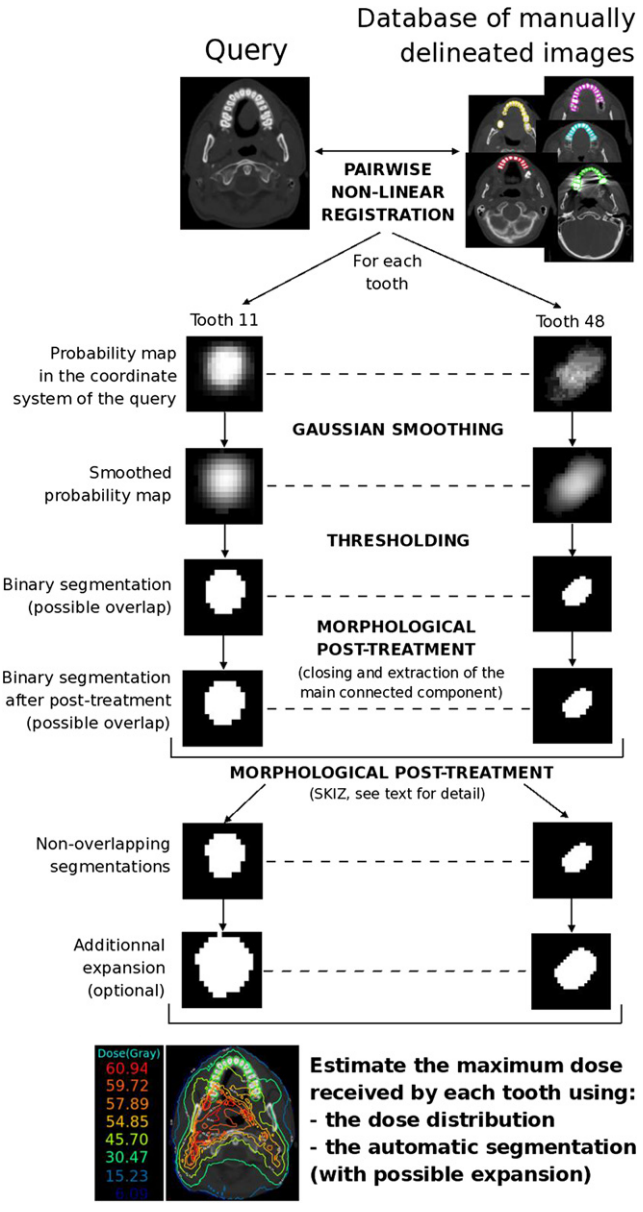

Fig. 2. Overview of the method. SKIZ = Skeleton by Influence Zones.

Evaluation of the framework

For dosimetric decision making, a worst-case scenario was assumed: the maximal dose to a particular tooth was considered representative of the dose to the root. The dose to the root was indeed representative of the dose to the underlying bone (mandible or maxilla).

The IMRT treatment planning was performed with the "anisotropic analytical algorithm" pencil-beam dose calculation in the Eclipse treatment planning system (Varian Medical Systems, Palo Alto, CA). The RT dose files were then imported into the ISOgray treatment planning system (DOSIsoft, Cachan, France) for structure delineation and dose analysis. The manual contours were delineated by means of ISOgray tools, and the automatic contours were obtained with the proposed method. The dose estimations in each delineated structure were compared in ISOgray. For each segmented volume, doses in a dense random sampling of points within the volume were computed on the basis of the 3D imported dose matrices. For instance, the doses for a tooth—which volume is approximately 1 cm^3—were computed in approximately 3000 points at random positions. From these dose points, DVHs and the maximal punctual dose were deduced. With this framework, the precision of the maximum punctual dose is approximately 3%.

To evaluate our framework, we applied a leave-one-out protocol to 8 IMRT patient images among the 21 of our database. We restricted the evaluation to IMRT patients to show that our method was both efficient and accurate in situations with steep gradients and complex dose distributions. Each original image was successively picked out from the initial database, and 40 images (after symmetrization of the 20 remaining images) were considered as "training data" to apply the proposed multi-atlas framework. The framework provided automatic segmentations of the teeth, mandible, and maxilla.

The validation was performed by comparing (*1*) the dose estimated visually from archived dosimetry without dental delineation,

with (*2*) the dose calculated from dental structures delineated manually, and with (*3*) the dose calculated from automatically segmented dental structures. An *a priori* 5-Gy accuracy was considered sufficient and relevant for the routine use of Dentalmaps. This quite mathematically precise *a priori* 5-Gy accuracy was chosen to account for the steep IMRT gradients and precise IMRT dose distributions, although it is yet uncertain whether we will ever have sufficient data to discriminate dose risk levels of strata of more than approximately 5–10-Gy thickness (compared with empiric risk strata of <40, 40–60, >60 Gy) (16). Qualitative and quantitative evaluations were carried out.

RESULTS

Qualitative evaluation

Visual comparisons between automatic and manual contours are presented at the level of the maxilla and mandible in Fig. 3. The global size and position of the teeth were well estimated using the automatic multi-atlas–based delineation method. The main differences between the manual and automatic contours were local differences on mandibular molars (data not shown).

Quantitative evaluation

Evaluation in terms of segmentation accuracy. Although the aim of this work was not the segmentation itself but dose estimate, we first checked segmentation accuracy. Indeed, segmentation accuracy and accurate dose estimate are closely related. We compared automatic contours with manual contours, and also investigated the effect of adding expansion to automatic contours on accuracy. We tested expansions of 1, 2, and 3 mm. As quantitative metrics, we used the Dice index, which quantifies the overlap between two contours, and the Hausdorff distance, which quantifies the worst surface-to-surface distance between two contours. The most accurate results were obtained using automatic contours with 1-mm expansion: average Dice coefficient and Hausdorff distance were 0.67 and 3.67 mm, respectively (total number of teeth was 214). Two-tailed paired *t* tests were performed. The difference between automatic contours without expansion and those with 1-mm expansion was significant for the Dice index ($p = 2.10^{-16}$) but not for the Hausdorff distance ($p = 0.15$). Accuracy dropped as the expansion increased from 1 to 3 mm. This was significant for both the Dice index and Hausdorff distance ($p \approx 10^{-14}$).

Comparison of dose estimations using different methods (visual, with manual contours, and with automatic contours provided by Dentalmaps). We evaluated the method accuracy for each test-patient tooth using DVHs, and in particular the maximum dose. A punctual maximal dose was chosen as the criteria to correlate the dose and the effect of radiation on dental structures. This decision was based on the CT slice thickness (2.5 mm) and on prior description of difficulties for automatic segmentation of small organs like the pituitary gland (17), we considered as ground truth the maximum doses estimated from manual contours (called D_{gt}). We compared ground truth with (*1*) maximum doses called D_{visu} estimated visually without any contour by the radiation oncologist (J.T.), who was unaware of estimates with manual and automatic contours, and with (*2*) maximum doses estimated using automatic contours (called D_{auto}) with or without additional expansions of 1, 2, or 3 mm (called $D_{auto+1mm}$, $D_{auto+2mm}$, and $D_{auto+3mm}$, respectively). To assess accuracy, we considered the difference $D - D_{gt}$ and its absolute value $|D - D_{gt}|$ for $D = D_{visu}$, D_{auto}, $D_{auto+1mm}$, $D_{auto+2mm}$, and $D_{auto+3mm}$. For each method, statistics on $D - D_{gt}$ and $|D - D_{gt}|$ were computed over all test-patient teeth (total number of teeth was 214). First, Fig. 4 shows the minimum, maximum, and average values of $D - D_{gt}$. This figure shows that visual estimation without any contour (in red) yielded the highest dose underestimation (−20.6 Gy) and the highest overestimation (+29.7 Gy) in comparison with ground truth. Moreover, visual estimation without any contour underestimated the maximum dose by 1.4 Gy on average. Automatic contours and their 1-mm expansion both provided smaller average under- and overestimation of the maximum dose (−0.4 Gy and +0.3 Gy, respectively), whereas the 2-mm and 3-mm expanded versions of the automatic contours clearly overestimated the maximum dose (+1.8 Gy and +2.7 Gy, respectively). These first results suggested that the optimal compromise between under- and

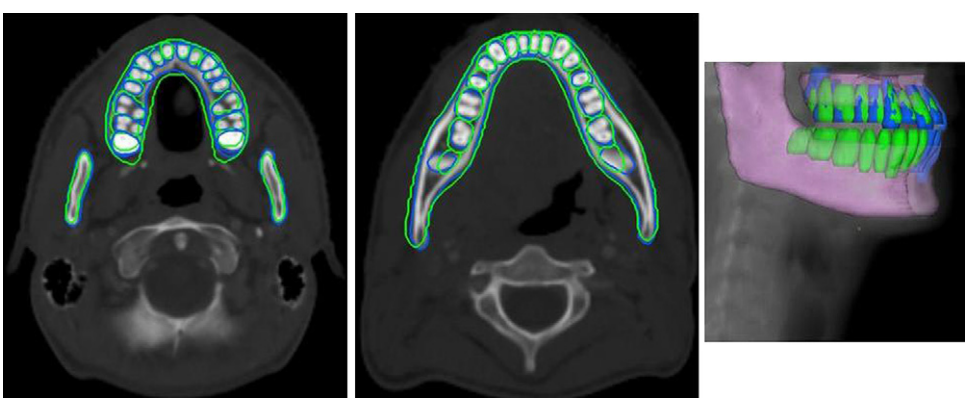

Fig. 3. Visual results at the level of the maxilla (left)/mandible (middle) of the automatic (in green) and manual segmentation (in blue) of the teeth, maxilla, and mandible for 1 patient. Right image: Three-dimensional reconstruction of the automatic (in green) and manual segmentation (in blue). Manual segmentation of the mandible and maxilla is represented in pink.

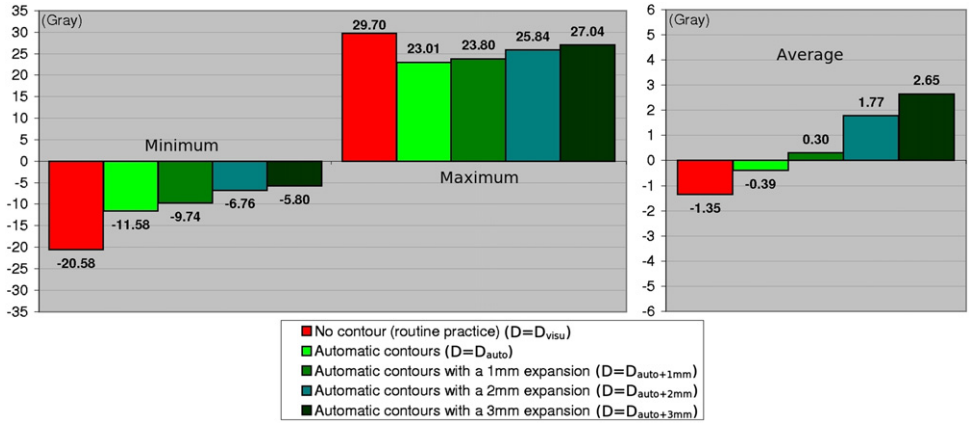

Fig. 4. Minimum, maximum, and average values of the estimation error $D - D_{gt}$ over all teeth of 8 test patients for $D = D_{visu}$, D_{auto}, $D_{auto+1mm}$, $D_{auto+2mm}$, and $D_{auto+3mm}$. The total number of values used for computing statistics was 214. D_{gt} = dose obtained with ground truth, *i.e.*, manual contours; D_{visu} = dose estimated visually without contours; D_{auto} = dose obtained with automatic contours.

overestimation of the maximum dose may fall within no expansion and a 1-mm expansion. These results were confirmed by the results in terms of absolute estimation error $|D - D_{gt}|$. Indeed, the 1-mm-dilated automatic-contour version provided the lowest absolute estimation error of the maximum dose (median value was 0.9 Gy). The difference with the other methods (D_{visu}, D_{auto}, $D_{auto+2mm}$, and $D_{auto+3mm}$) was statistically significant (all $p < 0.01$). Last, as illustrated in Fig. 5, the absolute estimation error using automatic contours with 1-mm expansion was within 2-Gy accuracy in 75% and within 5-Gy accuracy in 93% of the cases, respectively. By comparison, the absolute estimation error using visual estimation without any contour (which is routine practice procedure) was within 2-Gy accuracy in 30% of the cases only and within 5-Gy accuracy in 59% of the cases only. All these results confirmed the trend presented in the evaluation in terms of segmentation accuracy.

An example of DVHs obtained using manual and automatic contours with or without expansions is illustrated in Fig. 6. Maximal similarity with the manual contour-based DVHs was obtained with the DVHs provided with the automatic contours and their 1-mm expansion (solid light-green lines). Dose–volume histogram profiles obtained with automatic contour versions with 2-mm and 3-mm expansions were less relevant (dashed dark-green lines). Similar conclusions were yielded for DVHs of other teeth and other patients.

We also assessed the accuracy of our framework to estimate the maximum dose in the mandible and maxilla. For this evaluation, we had eight values for each structure

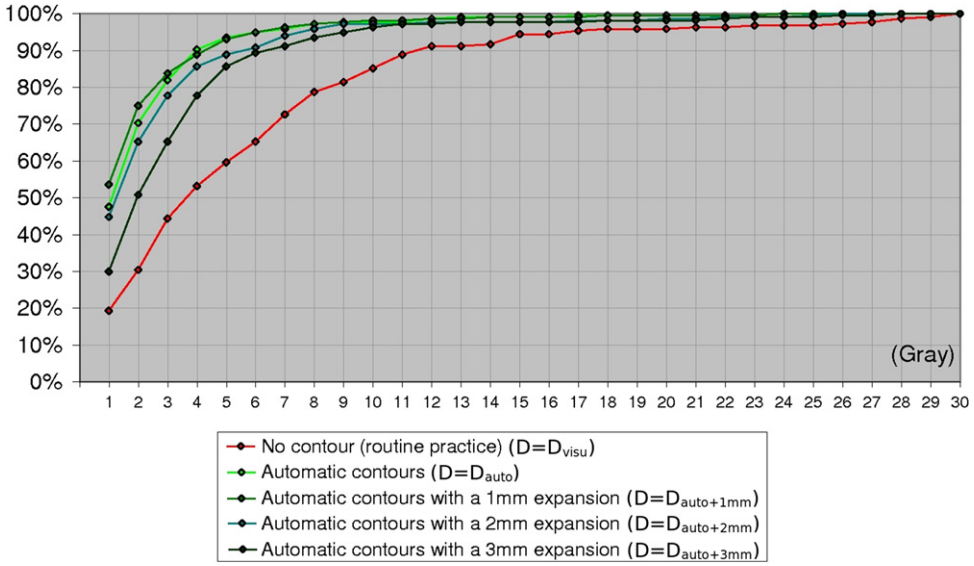

Fig. 5. For a given abscissa X, the ordinate values represent the percentages of cases for which the absolute estimation error $|D - D_{gt}|$ is smaller than X Gy (for $D = D_{visu}$, D_{auto}, $D_{auto+1mm}$, $D_{auto+2mm}$, and $D_{auto+3mm}$). For instance, the estimation error was less than 5 Gy in 59% of the cases with the visual method (red curve) and in 93% of the cases with automatic contours and automatic contours with 1-mm expansion. The total number of cases was 214 (all teeth of all 8 test patients).

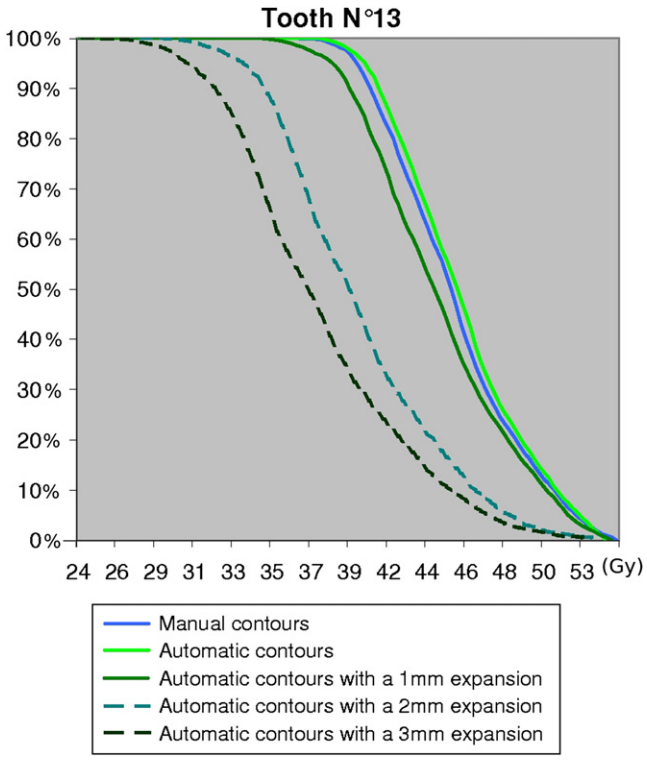

Fig. 6. Dose–volume histograms obtained for one tooth using the manual contours (blue line) and using the automatic contours without or with expansions of 1, 2, and 3 mm.

(compared with 214 values for the teeth). For both structures, automatic contours without expansion provided the most accurate results compared with manual contours, with worst-case estimation errors $D - D_{gt}$ remaining within the range [−1 Gy; +1 Gy] for all 8 test patients. An evaluation in terms of segmentation accuracy (Dice index and Hausdorff distance) was also carried out and led to the same conclusion.

DISCUSSION

Visual dose estimation may underestimate or overestimate the maximal dose, therefore potentially providing inaccurate risk-level data reported to the dentist. A dose–volume correlation in the order of 1 cm^3 of mandible receiving more than 70 Gy (18) has been associated with a risk of ORN. Additionally, it is usually considered that there is a high risk of posttraumatic ORN (65% of ORN cases) after 60 Gy, especially in posterior segments of the mandible (16). The scarcity of collateral arteries, radiation-induced endarteritis, and the 3H (hypovascularization, hypocellularity, hypoxia) or 2I hypotheses (infection, ischemia) have also been used to explain cases of mandibular ORN. There are hardly any data for the maxilla, despite the fact that implant failure has been reported in the anterior maxillary segment, a segment that may be exposed with IMRT anterior beam paths (12). The use of radiation techniques like IMRT is endowed with the potential to preserve the mandible. Preliminary results have suggested a potential for IMRT to reduce ORN rates (19). In the 1980s, we could note 1–10% of ORN in selected populations compliant with fluorides (20, 21) compared with 5–9% with conventional radiation therapy (22–24). Data are yet insufficient to clearly assess the benefit of new radiation techniques on the rate of carious lesions and ORN.

We also studied the tooth-by-tooth dose estimation accuracy. We were not able to compute significant statistics because we only had eight values or less for each tooth. Yet, we noticed less accurate results for molars (Teeth 16, 17, 18, 26, 27, 28, 36, 37, 38, 46, 47, and 48) in comparison with other teeth. This trend was found for segmentation accuracy (Dice index, Hausdorff distances) and maximum dose estimates. It may be due to several reasons. First, molars were more frequently missing in our database. There were therefore fewer manual segmentations available to estimate the segmentation of the query for these teeth, possibly resulting in lower accuracy. Second, wisdom teeth (18, 28, 38, and 48) were missing for approximately 3 out of 4 patients in the database. This prevalence seems similar to that found in the general population (unerupted teeth, missing teeth) or slightly higher here owing to dental extractions before radiotherapy. Therefore, registrations between one image with wisdom teeth and another image without wisdom teeth happened quite often. Such registrations may introduce an artificial spatial shift in the area around the wisdom teeth, which may result in lower segmentation accuracy for the neighboring teeth (*i.e.*, X6 and X7 [16, 17, 26, 27, 36, 37, 46, 47]). A way to overcome this limitation would be to split the database into patients with and without wisdom teeth and to use only the appropriate subset of images for segmenting a new query. However, a larger database would be required to implement this solution to have enough images in both subsets. Last, the lower accuracy obtained for the molars may be due to more frequent dental artifacts for these teeth and to a higher interindividual anatomic variability (number of roots and their shape). This variability cannot be entirely compensated with nonlinear registration.

Despite these limitations, the accuracy of this atlas-based framework appears relevant in routine practice. The risk for ORN after extraction and for implant failure is provided within 2-Gy accuracy, and with the postulate that the maximal dose to dental structures is representative of the dose to the root (*i.e.*, of the dose to the underlying bone, indeed). Furthermore, according to International Commission on Radiation Units and Measurements Report 83 recommendations, the maximal dose to a given OAR may be more reliably calculated on a given small volume (usually 2%) of this OAR, provided this OAR is entirely delineated. Mean dental volume was 1 cm^3, and only 7 teeth out of 214 were bigger than 2 cm^3 in our 8 test patients. The relevant maximal dose to a partial volume (Dnear max) to such small OARs as teeth remains to be determined. The certainty with which a treatment planning system can calculate the dose to a 1 × 1 × 1-cm^3 voxel or 2% of the OAR volume will be determined during the validation step.

Tooth	Dm (Gy)	ORN	Imp	Tooth	Dm (Gy)	ORN	Imp	Tooth	Dm (Gy)	ORN	Imp	Tooth	Dm (Gy)	ORN	Imp
Right maxilla				Left maxilla				Left mandible				Right mandible			
11	12			21	10			31	18			41	30		
12	12			22	12			32	30			42	34		
13	14			23	13			33	35			43	45		
14	17			24	18			34	48			44	48		
15	18			25	32			35	52			45	36		
16	18			26	34			36	65			46	36		
17	25			27	54			37	69			47	36		
18	20			28	60			38	71			48	34		

Fig. 7. Dose risk-level table, a simple tool to guide dentists when planning extractions or implants. Maximal doses (Dm) per tooth are provided, as well as risk-level color codes: black: unacceptable risk; red: high risk; black and white: moderate risk; green: no risk (16).

Although dental segmentation might also be done manually, the automation will facilitate prospectively providing a summary recording the dose and risk level for future use. The dental-based mandibular cartography obtained using the proposed framework is a practical tool to estimate the maximal dose. However, it is possible that DVHs of the horizontal portion of the mandible are more relevant than DVHs of the whole mandible to better assess the risk of ORN. The mandibular segmentations of the database can possibly be split into two portions, to provide an automatic segmentation of the horizontal portion instead of the whole mandible. The training data used in the proposed framework were patients immobilized with a nine-point thermoplastic mask without bite blocks. The impact of the bite-block immobilization technique has not been assessed. Additionally, this version with 1-mm expansions might be improved using a larger patient databank with thinner-slice planning CT.

Overall, our multi-atlas–based framework provided a reliable dental dosimetry and therefore a mandibular and maxillary dosimetric cartography. It is generally inferred that the risk of ORN is high after 60 Gy, moderate between 40 and 60 Gy, and mild or null below 40 Gy (16). This is also dependent on the location on the maxilla or mandible (mandible being more at risk) and the segment (posterior being more at risk) (4). However, it does not take into account other potential risk factors, like diabetes mellitus, vascular disease, concomitant chemotherapy, targeted therapies like anti-Epidermal Growth Factor Receptor (EGFR) or antiangiogenic therapies, and biphosphonates. Although the practical cut-points (risk classes) have been roughly established empirically on 2D data (16) without any knowledge of precise dental dose cartography (and with disclaimers regarding data certainty), they can be disseminated for research purposes. They should be taken with caution for clinical application in individual cases by clinicians using judgment. These putative risk classes should be the basis to provide a full dose–response risk curve made from high-quality data points from real cases collected prospectively using Dentalmaps. Our atlas-based framework is likely to provide better correlates between dental dose cartography and the occurrence of complications.

Another potential benefit of this atlas-based framework is the possibility to analyze dosimetric problems due to dental artifacts. Dental artifacts are common and result in inaccurate dosimetry with inaccurate dose calculation by most software and overlooked backscatter to mucosa (25). Dental delineation with application of virtual Hounsfield units to certain teeth in case of dental fillings might provide a means for more accurate adjusted dosimetry with real dental material density. It will, however, not solve the problem of uncertainties with target volume delineation (26–29). Artifacts surrounding dental fillings may be better managed with optimized retro-projection algorithms. This atlas-based framework would also be useful to dentists before irradiation: it might help them predict which teeth to spare or extract, depending on a provisional dosimetry. Further work is required to define the limits of validity in that setting.

Finally, Dentalmaps provides a relevant dose estimate to predict the risk of implant failure or the risk of ORN after dental extraction. Although it must be used with caution, Dentalmaps results may be given as a risk classes table that can be stored in the electronic patient chart or printed on a card of the size of a credit card for the patient or the dentist (Fig. 7). The validity of this risk estimate table will have to be reassessed prospectively. Validation studies of Dentalmaps are under way on a multicenter basis on patients extrinsic to the database within the Groupe d'Oncologie Radiothérapie des tumeurs de la Tête Et du Cou (www.gortec.org), first in patients with oropharyngeal tumors. The performances of Dentalmaps will also be tested in patients with oral cavity tumors and bite-block immobilization.

Despite several limitations, the principle of an automatic dental segmentation method provides a very attractive user-friendly interface between radiation oncologists and dentists. It has an interesting potential to prospectively establish dose–risk correlations when planning dental extractions or implant. It also has the potential to yield better dose–response data regarding ORN. The proposed framework is currently being integrated into the radiotherapy planning software ISOgray, commercialized by DOSIsoft.

CONCLUSIONS

Dose estimates using the Dentalmaps multi-atlas–based framework are more practical and relevant for the routine use than retrospective data collection, because manual

delineation of all dental structures is not feasible in routine practice. Importantly, the segmentation method used is less sensitive to artifacts (due to dental fillings) than average atlas methods. The accuracy of the dose estimation using the atlas is within 2-Gy accuracy. Dentalmaps seems a relevant interface in routine practice for radiation oncologists and dentists. Prospective multicenter assessment of the atlas is underway on patients extrinsic to the initial patient bank within the Groupe d'Oncologie Radiothérapie des tumeurs de la Tête Et du Cou.

REFERENCES

1. Delanian S, Chatel C, Porcher R, *et al*. Complete restoration of refractory mandibular osteoradionecrosis by prolonged treatment with a pentoxifylline-tocopherol-clodronate combination (PENTOCLO): A phase II trial. *Int J Radiat Oncol Biol Phys,* 2010 July 15.
2. Ozen J, Dirican B, Oysul K, *et al*. Dosimetric evaluation of the effect of dental implants in head and neck radiotherapy. *Oral Surg Oral Med Oral Pathol Oral Radiol Endod* 2005; 99:743–747.
3. Thariat J, De Mones E, Darcourt V, *et al*. [Teeth and irradiation in head and neck cancer]. *Cancer Radiother* 2010;14:128–136.
4. Thariat J, de Mones E, Darcourt V, *et al*. [Teeth and irradiation: Dental care and treatment of osteoradionecrosis after irradiation in head and neck cancer]. *Cancer Radiother* 2010;14: 137–144.
5. Thariat J, Ramus L, Darcourt V, *et al*. Compliance with fluoride custom trays in irradiated head and neck cancer patients. *Support Care Cancer* in press.
6. Epstein JB, van der Meij EH, Emerton SM, *et al*. Compliance with fluoride gel use in irradiated patients. *Spec Care Dentist* 1995;15:218–222.
7. Epstein JB, van der Meij EH, Lunn R, *et al*. Effects of compliance with fluoride gel application on caries and caries risk in patients after radiation therapy for head and neck cancer. *Oral Surg Oral Med Oral Pathol Oral Radiol Endod* 1996; 82:268–275.
8. Epstein J, van der Meij E, McKenzie M, *et al*. Postradiation osteonecrosis of the mandible: A long-term follow-up study. *Oral Surg Oral Med Oral Pathol Oral Radiol Endod* 1997; 83:657–662.
9. Epstein JB, Wong FL, Stevenson-Moore P. Osteoradionecrosis: Clinical experience and a proposal for classification. *J Oral Maxillofac Surg* 1987;45:104–110.
10. Eisbruch A, Ten Haken RK, Kim HM, *et al*. Dose, volume, and function relationships in parotid salivary glands following conformal and intensity-modulated irradiation of head and neck cancer. *Int J Radiat Oncol Biol Phys* 1999;45:577–587.
11. Nutting C, A'Hern R, Rogers MS, *et al*. First results of a phase III multicenter randomized controlled trial of intensity modulated (IMRT) versus conventional radiotherapy (RT) in head and neck cancer (PARSPORT: ISRCTN48243537; CRUK/03/ 005) (Abstr.). *J Clin Oncol* 2009;27:LBA6006.
12. Rosenthal DI, Chambers MS, Fuller CD, *et al*. Beam path toxicities to non-target structures during intensity-modulated radiation therapy for head and neck cancer. *Int J Radiat Oncol Biol Phys* 2008;72:747–755.
13. Commowick O, Gregoire V, Malandain G. Atlas-based delineation of lymph node levels in head and neck computed tomography images. *Radiother Oncol* 2008;87:281–289.
14. Guimond A, Meunier J, Thirion JP. Average brain models: A convergence study. *Comput Vis Image Underst* 2000;77:192–210.
15. Garcia V, Commowick O, Malandain G. A robust and efficient block matching framework for non linear registration of thoracic CT images. Paper presented at the Miccai Workshop on Grand Challenges in Medical Image Analysis; September 24, 2010; Beijing, China.
16. Gourmet R, Chaux-Bodard AG. [Tooth extraction in irradiated areas]. *Bull Cancer* 2002;89:365–368.
17. Isambert A, Dhermain F, Bidault F, *et al*. Evaluation of an atlas-based automatic segmentation software for the delineation of brain organs at risk in a radiation therapy clinical context. *Radiother Oncol* 2008;87:93–99.
18. Studer G, Studer SP, Zwahlen RA, *et al*. Osteoradionecrosis of the mandible: Minimized risk profile following intensity-modulated radiation therapy (IMRT). *Strahlenther Onkol* 2006;182:283–288.
19. Ben-David MA, Diamante M, Radawski JD, *et al*. Lack of osteoradionecrosis of the mandible after intensity-modulated radiotherapy for head and neck cancer: Likely contributions of both dental care and improved dose distributions. *Int J Radiat Oncol Biol Phys* 2007;68:396–402.
20. Horiot JC, Schraub S, Bone MC, *et al*. Dental preservation in patients irradiated for head and neck tumours: A 10-year experience with topical fluoride and a randomized trial between two fluoridation methods. *Radiother Oncol* 1983;1:77–82.
21. Horiot JC, Wambersie A. [Prevention of caries and of osteoradionecrosis in patients irradiated in oncology]. *Rev Belge Med Dent* 1991;46:72–86.
22. Tsai J, Lindberg ME, Garden AS, *et al*. Osteoradionecrosis and radiation dose to the mandible in oropharyngeal cancer (Abstr.). *Int J Radiat Oncol Biol Phys* 2010;78:S153.
23. Gomez DR, Zhung JE, Gomez J, *et al*. Intensity-modulated radiotherapy in postoperative treatment of oral cavity cancers. *Int J Radiat Oncol Biol Phys* 2008;73:1096–1103.
24. Peterson DE, Doerr W, Hovan A, *et al*. Osteoradionecrosis in cancer patients: The evidence base for treatment-dependent frequency, current management strategies, and future studies. *Support Care Cancer* 2010;18:1089–1098.
25. Rosengren B, Wulff L, Carlsson E, *et al*. Backscatter radiation at tissue-titanium interfaces. Analyses of biological effects from 60Co and protons. *Acta Oncol* 1991;30:859–866.
26. Baek CH, Chung MK, Son YI, *et al*. Tumor volume assessment by 18F-FDG PET/CT in patients with oral cavity cancer with dental artifacts on CT or MR images. *J Nucl Med* 2008;49: 1422–1428.
27. Kim Y, Tome WA, Bal M, *et al*. The impact of dental metal artifacts on head and neck IMRT dose distributions. *Radiother Oncol* 2006;79:198–202.
28. Nahmias C, Lemmens C, Faul D, *et al*. Does reducing CT artifacts from dental implants influence the PET interpretation in PET/CT studies of oral cancer and head and neck cancer? *J Nucl Med* 2008;49:1047–1052.
29. O'Daniel JC, Rosenthal DI, Garden AS, *et al*. The effect of dental artifacts, contrast media, and experience on interobserver contouring variations in head and neck anatomy. *Am J Clin Oncol* 2007;30:191–198.